Contrast Sensitivity of the

HUMAN EYE

and Its Effects on Image Quality

Peter G. J. Barten

SPIE OPTICAL ENGINEERING PRESS
A Publication of SPIE—The International Society for Optical Engineering
Bellingham, Washington USA

Chapter 3

Model for the spatial contrast sensitivity of the eye

3.1 Introduction

In the previous chapter, equations were given for the effect of noise on contrast sensitivity. In this chapter, these equations will be used for a model of the spatial contrast sensitivity of the eye. This model is based on the assumption that the contrast sensitivity is mainly determined by the internal noise generated in the visual system. For this model, additional assumptions have to be made about the optical properties of the eye and about the neural processing of the information. In this way, a quantitative description of the contrast sensitivity function will be obtained that also explains the dependence of contrast sensitivity on luminance and field size. The predictions by this model will be compared with a large number of published measurements of the contrast sensitivity. These measurements are usually made at medium and high luminance, which condition is called *photopic vision* (= daylight vision), but are sometimes also made at low luminance, which condition is called *scotopic vision* (= night vision). At photopic vision the cones act as photo-receptors, whereas at scotopic vision the rods act as photo-receptors. For practical reasons, the application of the model is restricted to photopic vision.

In the model, use will be made of the *modulation transfer function* or MTF. This function describes the filtering of the modulation by an image forming system as a function of the spatial frequency. The use of an MTF has the advantage that according to the convolution theorem, the MTFs of different parts of an image forming system can simply be multiplied with each other to obtain the total effect on the image. See, for instance, Papoulis (1968, p. 74). The MTF is based on the application of Fourier analysis and can, therefore, only be applied to linear systems. However, as the model is based on threshold signals and the system may be assumed to be linear around the threshold, nonlinearity effects may be neglected. From a comparison of the model with measured data, it appears that this neglect is justified.

3.2 Outline of the model

In the model, it is assumed that a luminance signal that enters the eye is first filtered by the optical MTF of the eye and then by the MTF of a lateral inhibition process. It is further assumed that the optical MTF is mainly determined by the eye lens and the discrete structure of the retina, and that the MTF of the lateral inhibition is determined by neural processing. For a comparison of the signal with the internal noise, Eq. (2.20) in Chapter 2 has to be modified into

$$m_t\, M_{opt}(u)\, M_{lat}(u) = k m_n \tag{3.1}$$

where $M_{opt}(u)$ is the optical MTF of the eye, $M_{lat}(u)$ is the MTF of the lateral inhibition process and m_n is the average modulation of the internal noise. After applying Eq. (2.43) to m_n at the right-hand side of this equation, one obtains

$$m_t\, M_{opt}(u)\, M_{lat}(u) = 2\,k \sqrt{\frac{\Phi_n}{XYT}} \tag{3.2}$$

where Φ_n is the spectral density of the internal noise and X, Y, and T are the spatial and temporal dimensions of the object, where the limited integration area of the visual system has to be taken into account by using Eqs. (2.48), (2.49), and (2.45), respectively, for these quantities.

Internal noise is partly due to photon noise caused by statistical fluctuations of the number of photons that generate an excitation of the photo-receptors, and partly due to neural noise caused by statistical fluctuations in the signal transport to the brain. Although the original image already contains photon noise before entering the eye, photon noise is not considered here as external noise, but as internal noise. This treatment might be clear from the fact that the spatial frequency components of this noise are not filtered by the lowpass filter formed by the eye lens. The spectral density of the internal noise may, therefore, be written in the form

$$\Phi_n = \Phi_{ph}\, M_{lat}^2(u) + \Phi_0 \tag{3.3}$$

where Φ_{ph} is the spectral density of the photon noise, and Φ_0 is the spectral density of the neural noise. In this equation, it is assumed that the photon noise is filtered together with the signal by the lateral inhibition process.

Fig. 3.1 shows a block diagram of the model. For completeness, external noise is also mentioned in this figure. External noise can, for instance, consist of display noise present in a television image, or of grain noise present in a photographic image. The spectral noise density of this external noise adds to the spectral noise density of the internal noise after multiplication by $M_{opt}^2(u)M_{lat}^2(u)$. However, in most of the cases treated in this chapter no external noise is present.

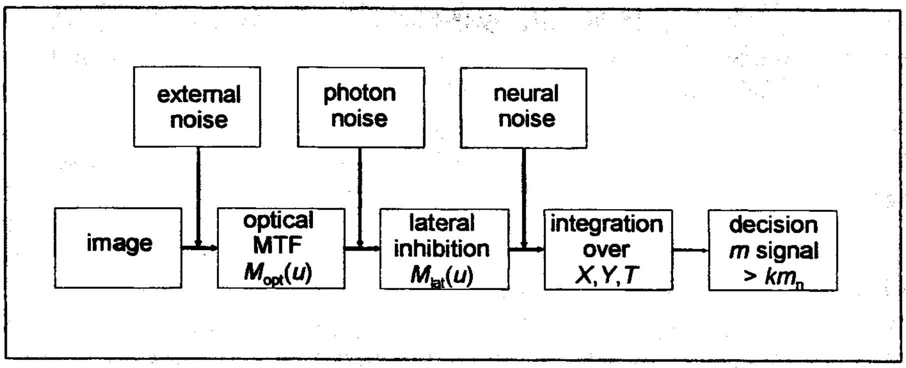

Figure 3.1: Block diagram of the processing of information and noise according to the contrast sensitivity model described here.

Insertion of Eq. (3.3) in Eq. (3.2) gives

$$m_t\, M_{opt}(u)\, M_{lat}(u) \;=\; 2\,k\,\sqrt{\frac{\Phi_{ph}\, M_{lat}^{\;2}(u) \;+\; \Phi_0}{XYT}} \tag{3.4}$$

The contrast sensitivity S, which is the inverse of the modulation threshold m_t, is then given by

$$S(u) \;=\; \frac{1}{m_t(u)} \;=\; \frac{M_{opt}(u)}{2k}\sqrt{\frac{XYT}{\Phi_{ph} \;+\; \Phi_0/M_{lat}^{\;2}(u)}} \tag{3.5}$$

This expression forms the basis of the given contrast sensitivity model given here. The various components of this expression will be treated in more detail in the following sections.

3.3 Optical MTF

The optical MTF used in the model does not include only the optical MTF of the eye lens, but also the effects of stray light in the ocular media, diffusion in the retina and the discrete structure of the photo-receptors. These effects have to be convolved with each other to obtain the total effect. For many convolutions in succession, the *central limit theorem* may be applied. See, for instance, Papoulis (1968, pp. 78-80). This theorem says that the total effect of several lowpass MTFs can be described by a Gaussian function. Therefore, it is assumed here that the optical MTF of the eye can be described by the following function:

$$M_{opt}(u) = e^{-2\pi^2\sigma^2u^2} \tag{3.6}$$

where σ is the standard deviation of the line-spread function resulting from the convolution of the different elements of the convolution process. That a Gaussian function forms a good approximation of the optical MTF of the eye, appears from a comparison of the high frequency behavior of the model with the measured data that will be given in section 3.9.

The quantity σ in Eq. (3.6) generally depends on the pupil diameter d of the eye lens. For very small pupil diameters, σ increases inversely proportionally with pupil size because of diffraction, and for large pupil diameters, σ increases about linearly with pupil size because of chromatic aberration and other aberrations. See Vos et al. (1976, Fig. 3). According to these authors, diffraction effects become noticeable only at pupil diameters smaller than 2 mm. Therefore, they may be neglected under normal viewing conditions. Therefore, it is assumed here that the dependence on pupil size can simply be expressed by the following equation:

$$\sigma = \sqrt{\sigma_0^2 + (C_{ab}\,d)^2} \tag{3.7}$$

where σ_0 is a constant, C_{ab} is a constant that describes the increase of σ at increasing pupil size, and d is the diameter of the pupil. From an evaluation of contrast sensitivity measurements, it appears that for observers with good vision, σ_0 is about 0.5 arc min and C_{ab} is about 0.08 arc min/mm. The value of σ_0 is only partly determined by the optical effect of the eye lens. It is also determined by the density of the photoreceptors. As the density of the cones decreases with increasing distance from the center of the retina, σ_0 increases with this distance. See Chapter 4. However, for the normal situation of foveal vision treated in this chapter, σ_0 may be considered as constant.

The diameter d of the pupil generally depends on the average luminance of the observed object. To calculate the pupil size for a given luminance, the following simple approximation formula given by Le Grand (1969, p. 99) can be used:

$$d = 5 - 3\tanh(0.4\log L) \tag{3.8}$$

where d is the pupil diameter in mm and L is the average luminance in cd/m^2. This expression is similar to other formulae, earlier given by Crawford (1936), Moon & Spencer (1944) and De Groot & Gebhard (1952). These formulae represent an average of various measurement data that show a large spread. Apart from the difference between different observers, this spread is also caused by the difference in the angular size of the object fields used in the experiments. Bouma (1965) investigated the effect of different field sizes. From his measurements an approximately quadratic dependence on field size can be derived. By assuming that Eq. (3.8) is valid for an average field size of 40°×40°, one obtains the following approximation formula where also the field size is taken into account

$$d = 5 - 3\tanh\{0.4\log(LX_o^2/40^2)\} \tag{3.9}$$

where X_o is the angular field size of the object in degrees. For a rectangular field X_o^2 has to be replaced by X_oY_o, and for a circular field X_o^2 has to be replaced by $\pi/4 \times D^2$ where D is the field diameter in degrees. This expression will generally be used here as a refinement of Eq. (3.8). It is in fact only valid for young adult observers. At older ages, the pupil size decreases with age. See, for instance, Kumninck (1954, Fig. 4) and Bouma (1965, Fig. 7.30).

3.4 Photon noise

The effect of photon noise on the contrast sensitivity of the eye was first discovered by de Vries (1943) and was later evaluated by Rose (1948) who explicitly cites the paper of de Vries. Often an earlier paper of Rose (1942) is cited for this effect, but this paper does not contain any mention of this effect.

According to de Vries the detection threshold at low luminance levels is determined by fluctuations in the number of photons that cause an excitation of the photo-receptors. Let the number of these photons within an area $\Delta x \Delta y$ and time Δt be n. For the statistical process of the arbitrary arriving photons, the standard deviation of this number is equal to $\sqrt{\bar{n}}$ where $\bar{n}$ is the average value of n. This average value may be expressed in the average flux density j of the photons with the equation

$$\bar{n} = j\,\Delta x\,\Delta y\,\Delta t \tag{3.10}$$

For the relative standard deviation σ_n of n holds

$$\sigma_n = \frac{\sqrt{\bar{n}}}{\bar{n}} = \frac{1}{\sqrt{j\,\Delta x\,\Delta y\,\Delta t}} \tag{3.11}$$

According to de Vries these fluctuations form the background noise that hampers the observation of an object. Application of Eq. (2.42) gives for the spectral density of the photon noise

$$\Phi_{ph} = \sigma_n^2\,\Delta x\,\Delta y\,\Delta t \tag{3.12}$$

where σ_n has replaced σ_n and ϕ_{ph} has replaced ϕ_n. Inserting Eq. (3.11) in this expression gives

$$\Phi_{ph} = \frac{1}{j} \tag{3.13}$$

This equation says that the spectral density of photon noise is equal to the inverse of the average flux density of the photons on the retina that cause an excitation of the photo-receptors. The flux density on the retina can be derived from the luminous intensity of the light entering the eye with the following equation:

$$j = \eta p E \tag{3.14}$$

where η is the quantum efficiency of the eye, p is the photon conversion factor for the conversion of light units in units for the flux density of the photons and E is a quantity that describes the retinal illuminance. Each of these quantities will be treated in more detail in this section.

The quantum efficiency η is defined here as the average number of photons causing an excitation of the photo-receptors, divided by the number of photons entering the eye. Although the quantum efficiency varies in principle with the wavelength, the wavelength dependence will be taken into account in the photon conversion factor. See Appendix A of this chapter. In this way η represents the quantum efficiency at the maximum of the spectral sensitivity curve. Contrary to what one would expect, the quantum efficiency of the eye is very low. From an evaluation of contrast sensitivity measurements, it appears that η is about 3% or less (See, for instance, Table 3.1 in section 3.9.15). Van Meeteren (1978) found even values of 2% and less by measuring the contrast sensitivity with and without artificial image intensification. He tried to explain the low quantum efficiency by various causes of losses. A part of the light is lost by absorption in the ocular media, another part falls in the interstices between the photo-receptors, a part of the light falling on a photo-receptor is not absorbed, and finally not every absorbed photon causes an excitation. However, van Meeteren could not explain the low quantum efficiency that he measured by an estimate of these losses. The low quantum efficiency might be explained by fluctuations in the excitation of the photo-receptors. If these fluctuations are not negligible, they form an additional noise source that can be translated in an effectively lower quantum efficiency.

The photon conversion factor p in Eq. (3.14) is defined as the number of photons per unit of time, per unit of angular area, and per unit of luminous flux per angular area of the light entering the eye. Absorption losses and other losses are already taken into account in the quantum efficiency η. The number of photons generally depends on the spectral wave length of the light. Equations for the calculation of the photon conversion factor from the spectral composition of the light source are given in Appendix A of this chapter. They are derived from basic photometric and physical quantities. For the calculation of the photon conversion factor a distinction has to be made between photopic vision (= daylight vision) where the cones act as photo-receptor, and scotopic vision (= night vision), where the rods act as photo-receptor. The spectral sensitivity for photopic vision is different from that for scotopic vision, as the cones are less sensitive for blue light and the rods are less sensitive for red light. In Table 3.2 of Appendix A of this chapter, numerical values of the photon conversion factor are given for different light sources. Although the use of the contrast sensitivity model given here is restricted to photopic viewing, data for scotopic viewing are also given as general information.

The quantity E in Eq. (3.14) is proportional to the retinal illuminance and can be calculated from the luminance L of the object and the pupil size d with the following equation

$$E = \frac{\pi d^2}{4} L \tag{3.15}$$

If the pupil size is expressed in mm and the luminance in cd/m^2, E is given in Troland, indicated with Td. 1 Troland corresponds with a retinal illuminance of about 2×10^{-3} lux, taking into account the absorption of the light in the ocular media and the angular area of the pupil seen from the retina. Although the Troland does not have the dimension of illuminance, it is for practical reasons chosen as a measure of retinal illuminance. The transition between scotopic vision and photopic vision occurs at a level between 1 and 10 Td. The pupil size can be measured, or can be derived from the luminance with Eq. (3.9).

For the photopic viewing conditions used here, Eq. (3.15) has to be corrected for the Stiles-Crawford effect. For light falling on the cones, Stiles & Crawford (1933) found that rays entering near the edge of the pupil are visually much less effective than rays near the center of the pupil. From the work by Stiles and Crawford, Moon & Spencer (1944) and Jacobs (1944) derived an expression that forms a modification of Eq. (3.15) and may be written in the following form:

$$E = \frac{\pi d^2}{4} L \{ 1 - (d/9.7)^2 + (d/12.4)^4 \} \tag{3.16}$$

where d is expressed in mm. This expression will be used in the model. Although the decrease of the quantum efficiency by the Stiles-Crawford effect could also have been taken into account in the quantum efficiency η, the use of this expression is preferred here for practical reasons. For large pupil sizes, the correction for the Stiles-Crawford effect can amount to 50%.

By combining Eqs. (3.13) and (3.14) one obtains

$$\Phi_{ph} = \frac{1}{\eta p E} \tag{3.17}$$

According to this equation and Eq. (3.5), contrast sensitivity increases at low luminance levels with the square root of retinal illuminance. At these levels the effect of photon noise is so large that the effect of neural noise may be neglected. This square root behavior is known as *de Vries-Rose law*. An example of this behavior will be shown by the measurement data given in Fig. 3.21 of section 3.9.13.

3.5 Neural noise

In the model, it is assumed that neural noise is caused by statistical fluctuations in the signal transported to the brain. Contrary to electronic image systems, where usually only one wire is used for the transport of a signal, the image formed on the retina of the eye is transported to the brain by many fibers in parallel. When the image consists of a uniformly illuminated field, one may not expect that the different parts of this field will be reproduced by all nerve fibers in the same amount. Small differences between the different fibers will cause noise in the image arriving in the brain. The size of these differences can be estimated from the spectral density of the noise. From a comparison of contrast sensitivity measurements with the results obtained with the model, the spectral density Φ_0 of the neural noise may be estimated to be about 0.03×10^{-6} sec deg^2 (This follows, for instance, from the measurements shown in sections 3.9.11 and 3.9.12). From Eq. (2.42) follows for the relative standard deviation of the signal transported by an individual nerve fiber:

$$\sigma = \sqrt{\frac{\Phi_0}{\Delta x\,\Delta y\,\Delta t}} \tag{3.18}$$

where $\Delta x \Delta y$ is the retinal angular area covered by one nerve fiber, and Δt is the integration time of the visual system. The density of ganglion cells from which the nerve fibers originate may be estimated to be about 1,800 cells per deg^2 in the center of the retina (See section 4.2 of Chapter 4). This means that $1/(\Delta x \Delta y) \approx 1{,}800/\text{deg}^2$. If for the integration time of the eye a value of 0.1 sec is used, the relative standard deviation of the signal transported by the individual nerve fibres becomes

$$\sigma = \sqrt{\frac{0.03\cdot 10^{-6}\cdot 1{,}800}{0.1}} = 0.023$$

This is a fluctuation of 2.3%, which may be considered as a reasonable value.

In the model, it is assumed that neural noise does not depend on retinal illuminance. At high retinal illuminance levels where the effect of photon noise decreases, neural noise remains as only noise source. According to Eq. (3.5) contrast sensitivity then becomes independent of luminance. This behavior is known as *Weber's law*. An example of this behavior will be shown by the measurement data given in Fig. 3.21 of section 3.9.13.

3.6 Lateral inhibition

In our model, it is assumed that the luminance signal and the added photon noise are filtered in the neural system by a lateral inhibition process that attenuates low spatial frequency components. Since the contrast sensitivity appears to decrease linearly with the inverse of spatial frequency at low spatial frequencies, the effect of lateral inhibition can be characterized by an MTF that increases linearly with spatial frequency at low spatial frequencies up to 1 at a certain spatial frequency and remains further constant at higher spatial frequencies. From an investigation of natural scenes, Field (1987) found that the amplitude of the spatial frequency components of natural images decreases linearly with spatial frequency. This property of natural scenes is obviously compensated at low spatial frequencies by the increase of the MTF in this area due to the lateral inhibition. The existence of lateral inhibition may, therefore, probably be explained by the fact that the eye can make in this way a more efficient use of the dynamic range of signals that it can handle.

As was already supposed by Schade (1956) and was experimentally confirmed by Enroth-Cugell & Robson (1966) in their investigation with cats, lateral inhibition consists of the subtraction of a spatially lowpass filtered signal from a signal that is directly collected from the photo-receptors. Enroth-Cugell and Robson described the point-spread function of this process by a difference of two Gaussian functions, which has the form of a Mexican hat. This model is usually called *DOG model* (difference of Gaussians). However, it leads to a quadratic increase of contrast sensitivity at low spatial frequencies, whereas measurements of the contrast sensitivity clearly show a linear increase. Therefore, a different approach will be followed here.

From an evaluation of published contrast sensitivity measurements, we found that the MTF of the lateral inhibition process can well be described by the following approximation formula (Barten, 1992):

$$M_{lat}(u) = \sqrt{1 - e^{-(u/u_0)^2}} \qquad (3.19)$$

This function is shown by the solid curve in Fig. 3.2. It gives a linear increase of the MTF with spatial frequency up to a value 1 at a spatial frequency u_0 above which the lateral inhibition ceases. From a best fit of the model with the published contrast sensitivity measurements given in section 3.9, it appears that u_0 is about 7 cycles/deg. As contrast sensitivity is nearly independent of orientation, certainly at low spatial frequencies, it may further be assumed that the lateral inhibition process is rotationally symmetric.

As the MTF of the lateral inhibition process is the result of the subtraction of a lowpass filtered signal from a signal that is directly obtained from the photo-receptors, the MTF of the lateral inhibition process may also be described by

$$M_{lat}(u) = 1 - F(u) \qquad (3.20)$$

where $F(u)$ is the MTF of the spatial lowpass filter. Combination of Eqs. (3.19) and (3.20) gives

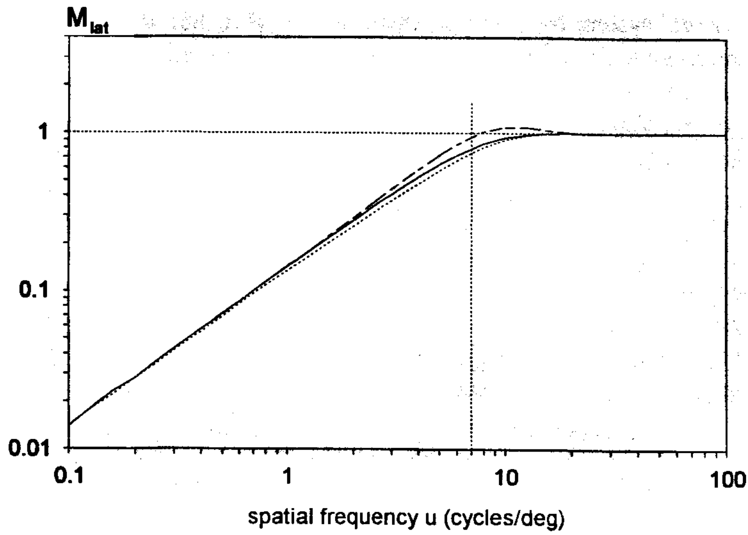

Figure 3.2: Solid curve: MTF of the lateral inhibition process given by Eq. (3.19) with u_0 = 7 cycles/deg. Dotted curve: MTF calculated with Eqs. (3.20) and (3.21) for the receptive field given by Eq. (3.23). Dashed curve: MTF calculated with Eqs. (3.20) and (3.25) for the annular receptive field given by Eq. (3.24).

$$F(u) = 1 - \sqrt{1 - e^{-(u/u_0)^2}} \tag{3.21}$$

The point-spread function that gives such an MTF can be found by an inverse Hankel transform of this expression. See, for instance, Papoulis (1968, pp. 140-145). The result can be numerically calculated but cannot be represented in mathematical form. This becomes, however, possible, if Eq. (3.21) is replaced by the following expression:

$$F(u) = 0.5\,e^{-2u/u_0} + 0.5\,e^{-(u/u_0)^2} \tag{3.22}$$

The MTF given by this function has nearly the same shape as the MF given by Eq. (3.19). It is shown by the dotted curve in Fig. 3.2. An inverse Hankel transformation of this function gives

$$f(r) = \frac{0.25\,\pi u_0^2}{(1 + \pi^2 u_0^2 r^2)^{3/2}} + 0.5\,\pi u_0^2\, e^{-\pi^2 u_0^2 r^2} \tag{3.23}$$

This function describes the *receptive field* of the inhibition process.

After the classical DOG model for the lateral inhibition process, a model consisting of a ring of Gaussians has been introduced. See, for instance, Young (1991). This model is called *DOOG model* (difference of offset Gaussians). These Gaussians form together an annular shaped lowpass filter, instead of the continuous Gaussian lowpass filter used in the DOG model. An annular lowpass filter seems to give a better description of the lateral inhibition process. The lowpass filter given by

Eq. (3.23) can be changed in an annular filter by modifying Eq. (3.23) into

$$f(r) = \frac{0.25\pi u_0^2}{(1+\pi^2 u_0^2 r^2)^{3/2}} + 1.5\pi u_0^2 e^{-\pi^2 u_0^2 r^2} - 1.75\pi u_0^2 e^{-1.75\pi^2 u_0^2 r^2} \tag{3.24}$$

A Hankel transform of this expression gives

$$F(u) = 0.5e^{-2u/u_0} + 1.5e^{-(u/u_0)^2} - 1.0e^{-\frac{1}{1.75}(u/u_0)^2} \tag{3.25}$$

This function gives a slightly different description of the MTF of the lateral inhibition process than Eq. (3.19). The MTF derived from this function is shown by the dashed curve in Fig. 3.2.

Fig. 3.3 shows a cross-section of the total point-spread function of the eye obtained by a combination of the optical point-spread function of the eye with the point-spread function of the annular lowpass filter given by Eq. (3.24). The shape of the annular lowpass filter is shown by the dotted curve in this figure, which is plotted with a negative sign to indicate the subtraction made by this filter. For u_0 the mentioned value of 7 cycles/deg is used. The figure further shows measurement data of the total point-spread function given by Blommaert et al. (1987). These data were obtained with a sophisticated perturbation technique based on peak detection of a combination of sub-threshold stimuli. The measurements were made with an artificial

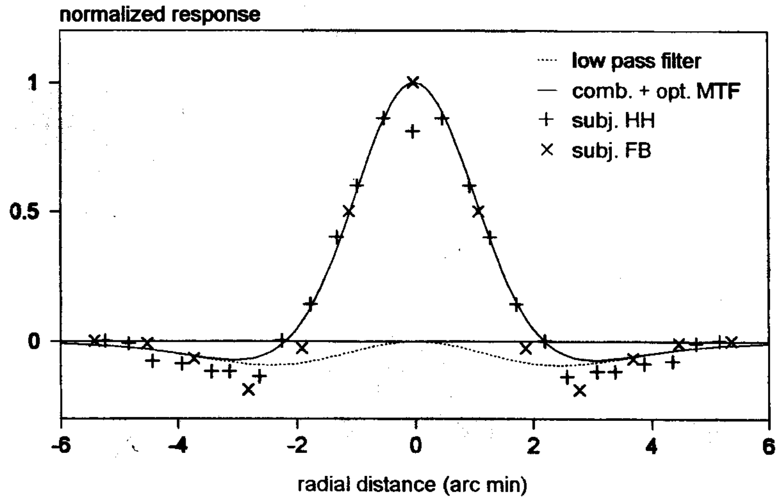

Figure 3.3: Solid curve: cross-section of the total point-spread function of the eye obtained by a combination of the optical point-spread function of the eye with the annular point-spread function of the low-pass inhibition filter given by Eq. (3.23). Dotted curve: cross-section of the annular point-spread function of the lowpass inhibition filter. Data points: measurements of the total point-spread function by Blommaert et al. (1987). For the calculation of the solid curve, the σ of the optical point-spread function has been adapted to the measurements.

pupil of 2 mm and a retinal illuminance of 1200 Td. The value used for σ in the calculated point-spread function has been adapted to the measurements and appears to be somewhat higher than the usual value of 0.5 arc min. Apart from this, the calculations reasonably agree with the measurements. However, the measurements show slightly deeper negative side lobes.

Although the annular filter might give a somewhat better description of the receptive field of the lateral inhibition process, still some uncertainties remain. Therefore, and for the sake of simplicity, still the simple formula given by Eq. (3.19) will be used in the model given here.

3.7 Monocular vision versus binocular vision

In comparing visual thresholds, it is important to take into account whether the observation is made with one eye, or with both eyes. At binocular vision, the information of both eyes is combined, while the internal noise of both eyes is not correlated, as the noise is separately generated in each eye. This can be considered as a doubling of the effective integration area. According to Eq. (2.43), the modulation of the internal noise is then reduced with a factor $\sqrt{2}$. So, the contrast sensitivity for binocular viewing increases with a factor $\sqrt{2}$ compared with monocular viewing. This holds only if the information of both eyes is completely combined, and if there is no noise added to the combined information processed in the brain. From measurements, it appears that this is indeed the case. Campbell & Green (1965) found that the contrast sensitivity for binocular viewing is a factor $\sqrt{2}$ higher than for monocular viewing and van Meeteren (1973) later also found the same results.

As binocular vision is the most common type of viewing, the factor $\sqrt{2}$ is used as standard in the contrast sensitivity model given here. The contrast sensitivity given by Eq. (3.5) has, therefore, to be multiplied with this factor. For monocular vision the contrast sensitivity is a factor $\sqrt{2}$ smaller. If the contrast sensitivity is limited by external noise, the noise presented to both eyes is correlated. Then the contrast sensitivity has also to be taken a factor $\sqrt{2}$ smaller. In this situation it makes no difference if the object is observed with one eye or with two eyes.

3.8 Complete model

After correcting Eq. (3.5) with a factor $\sqrt{2}$ for binocular viewing and after inserting Eq. (2.51) given in Chapter 2 and the equations given in the preceding sections, the following formula for the spatial contrast sensitivity function at binocular vision is obtained:

$$S(u) = \frac{1}{m_t(u)} = \frac{M_{opt}(u)/k}{\sqrt{\dfrac{2}{T}\left(\dfrac{1}{X_o^2}+\dfrac{1}{X_{max}^2}+\dfrac{u^2}{N_{max}^2}\right)\left(\dfrac{1}{\eta p E}+\dfrac{\Phi_0}{1-e^{-(u/u_0)^2}}\right)}} \qquad (3.26)$$

For monocular vision, $S(u)$ is a factor $\sqrt{2}$ smaller. This means that the factor 2 under the square root sign has to be replaced by 4. In this equation, $M_{opt}(u)$ is the optical MTF given by Eq. (3.6), u is the spatial frequency, k is the signal-to-noise ratio, T is the integration time of the eye, X_o is the angular size of the object, X_{max} is the maximum angular size of the integration area, N_{max} is the maximum number of cycles over which the eye can integrate the information, η is the quantum efficiency of the eye, p is the photon conversion factor that depends on the light source and is given in Table 3.2 in Appendix A of this chapter, E is the retinal illuminance in Troland, Φ_0 is the spectral density of the neural noise, and u_0 is the spatial frequency above which the lateral inhibition ceases. This formula holds for the situation that the object dimensions in x and y directions are equal. For nonequal dimensions, the factor between the brackets that contains the object size has to be replaced by $1/XY$ where X and Y are given by Eqs. (2.48) and (2.49), respectively. The constants in the model have the following typical values:

$k = 3.0$	$T = 0.1$ sec	$\eta = 0.03$
$\sigma_0 = 0.5$ arc min	$X_{max} = 12°$	$\Phi_0 = 3\times10^{-8}$ sec deg^2
$C_{ab} = 0.08$ arc min/mm	$N_{max} = 15$ cycles	$u_0 = 7$ cycles/deg

For T, it is assumed that the presentation time is long with respect to the integration time of the eye; otherwise Eq. (2.45) has to be used. The given constants are valid for an average observer, foveal vision and photopic viewing conditions. They have been obtained from a best fit with measurement data. For an arbitrary individual subject, only the values of σ_0, η, and k have to be adapted.

Fig. 3.4 shows the cumulative effect of various factors on the shape of the contrast sensitivity function. The figure has been calculated with Eq. (3.26) for a field size of 10°×10° using the given typical values of the constants. The horizontal line at the top of the figure shows the ultimate limit of the contrast sensitivity for this field size. This limit is determined by neural noise. Lateral inhibition causes a linear attenuation of this limit at low spatial frequencies. The maximum number of cycles causes a decay at high spatial frequencies, which is further enforced by the optical MTF of the eye. Photon noise causes a further decrease of the contrast sensitivity and a change in shape of the contrast sensitivity function at lower luminance levels. The figure shows that for low luminance and not too low spatial frequency, the contrast

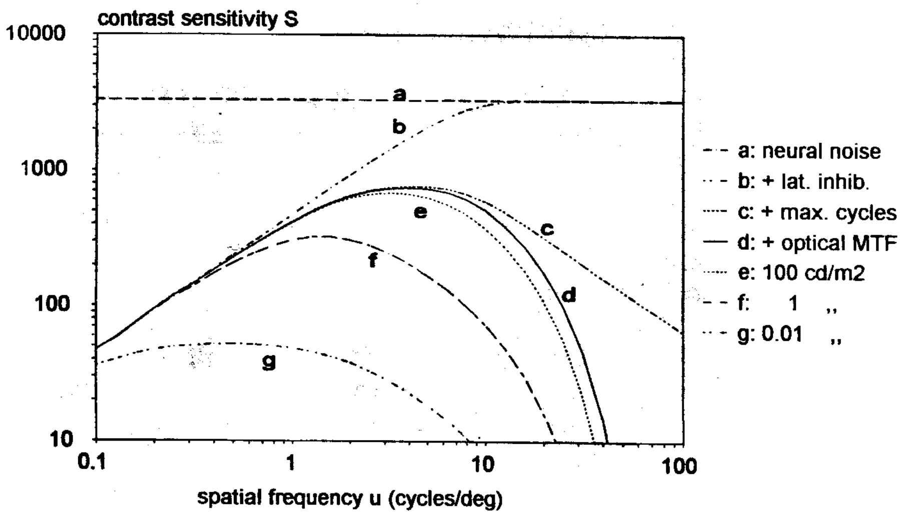

Figure 3.4: Cumulative effect of different factors on contrast sensitivity, calculated with Eq. (3.26) for a field size of 10°×10°: (a) neural noise; (b) + lateral inhibition; (c) + limited number of cycles; (d) + optical MTF; (e), (f), and (g) + photon noise at 100 cd/m^2, 1 cd/m^2, and 0.01 cd/m^2, respectively.

sensitivity increases with the square root of the luminance, according to the de Vries-Rose law. The figure also shows that for high luminance or low spatial frequency, the contrast sensitivity is nearly independent of the luminance, according to Weber's law. The dependence of contrast sensitivity on field size is not shown in the figure, but will later be shown in Figs. 3.19 and 3.22 where the model is compared with contrast sensitivity measurements for different field sizes. These figures show that the field size causes a vertical shift of the low frequency part of the curves, whereas the high frequency part remains the same, due to the effect of the limited number of cycles.